

Ultrafast optical nonlinearities of single gold nanorods

Matthew Pelton,* Mingzhao Liu, Sungnam Park, Norbert F. Scherer, and Philippe Guyot-Sionnest

*Department of Physics, Department of Chemistry, and James Franck Institute,
University of Chicago, 5640 S. Ellis Ave., Chicago, IL 60637*

(Dated: May 24, 2019)

We have measured third-order nonlinearities in the optical scattering from individual Au nanorods using an interferometric pump-probe technique. The nonlinearity produces changes of as much as 20% in the scattering cross-section over the 20-fs pulse duration. The magnitude of the ultrafast nonlinearity is the same as that due to heating of conduction electrons in the metal, suggesting the increased damping or saturation of strongly driven plasmons.

PACS numbers: 78.67.Bf, 78.47.+p

Conventional photonic devices are restricted by the diffraction limit to be larger than half the optical wavelength, limiting the possibilities for large-scale integration [1]. One possible way to overcome this limit is to couple light to surface plasmons in metal nanostructures, thereby confining optical fields to nanometer-scale dimensions [2]. Localization of electromagnetic fields around metal nanoparticles leads to strong enhancement of effects such as Raman scattering [3, 4], motivating the search for structures with the largest possible local field enhancements. At the same time, preliminary steps have been made towards using surface plasmons to construct nanometer-scale photonic devices, such as chains of nanoparticles that may serve as waveguides below the diffraction limit [5, 6]. Development of these applications will require an understanding of the optical nonlinearities of metal nanoparticles. For example, nonlinearities offer the possibility of controlling light propagation along nanoparticle chains, but may also limit achievable local field enhancements.

Previous measurements of metal-nanoparticle nonlinearities have generally involved large ensembles of particles [7, 8, 9, 10, 11], and the interpretation of the results has been complicated by the attendant distribution of particle sizes, shapes, and interactions. Isolating single particles removes the effects of inhomogeneous broadening, allowing the measurement of inherent nonlinearities of individual particles [12, 13]. Investigations of the coherent nonlinearities of surface plasmons are uncommon, though, and have not been extended to the single-particle level. Measuring such nonlinearities requires exciting and probing the particle on resonance with the plasmon frequency, and requires using ultrafast laser pulses whose duration is comparable to the rapid dephasing time of the plasmons.

In this Letter, we report the first investigations of resonant, ultrafast nonlinearities of surface plasmons in individual metal nanoparticles. In particular, we study nonlinearities from single rod-shaped Au nanoparticles [14, 15, 16]. These nanorods exhibit a strong longitudinal plasmon resonance, whose frequency is determined by the aspect ratio of the rods [17]. The rods are chemically syn-

thesized using a seed-mediated growth method [18, 19]. This method produces single crystals of Au with smooth surfaces, minimizing damping of the plasmon due to scattering. Damping due to interband transitions is reduced by selecting particles with a plasmon resonance near 1.55 eV [20]; this energy also matches the Ti:Sapphire laser used to excite and probe the rods.

The sample consists of a sparse sub-monolayer of rods, bound to a glass coverslip using a mercaptosilane coupling agent [21]. Optical measurements are made using

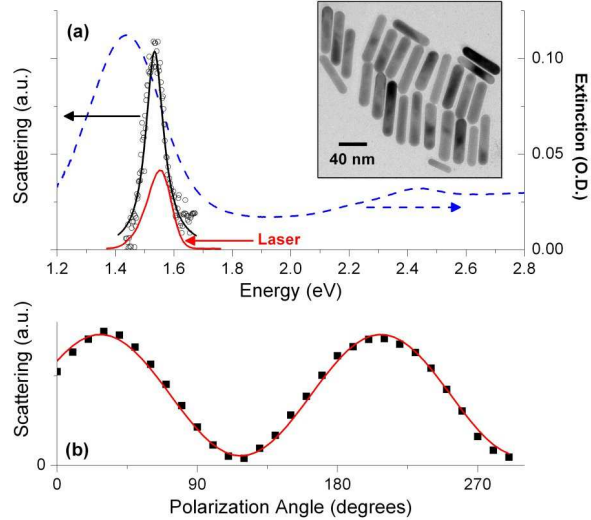


FIG. 1: (Color online) (a) The dashed line (blue online) is the measured extinction of an ensemble of Au nanorods in aqueous solution. The circles show the measured scattering spectrum from a single nanorod on a glass surface. The line through these points is the calculated scattering spectrum for a single rod with an aspect ratio of 5.25. The lower (red) curve shows the measured spectrum of the laser used to excite the rods. The inset shows Au nanorods imaged with a transmission-electron microscope (TEM). (b) The points are the measured intensity of laser light scattered off a single rod as the incident laser polarization is varied. The (red) line is a sinusoidal fit.

total-internal-reflection microscopy [22]. Incident excitation and probe light is focussed onto the sample through a glass prism. Light scattered by a nanorod is collected using a microscope objective and is imaged onto a multi-mode optical fiber, which effectively selects a $2 \mu\text{m}$ spot on the sample. For spectral measurements, the light is sent to a spectrometer equipped with a cooled CCD array detector (Andor); for time-resolved measurements, the light is sent to an avalanche photodiode (Hamamatsu).

Single rods can be identified by exciting with incoherent white light and measuring the spectrum of scattered light; a typical spectrum is shown in Fig. 1(a). Since the single rod is in air, attached to a glass surface, the plasmon resonance is blue-shifted by about 0.17 eV compared to that of rods in solution. The narrow, nearly Lorentzian peak in the measured scattering spectrum is an indication that the scattering comes from a single rod.

This was verified quantitatively by comparing to a theoretically calculated spectrum. The calculation is done in the quasi-static approximation [17], treating the rod as a prolate ellipsoid, and approximating the asymmetric environment of the rod as a homogeneous, transparent dielectric medium. The imaginary part of the dielectric function of Au is taken to be [23, 24, 25]

$$\epsilon_2(\omega, T_e) = \frac{\omega_p^2 \gamma(T_e)}{\omega [\omega_p^2 + \gamma(T_e)^2]} + \epsilon_2^{d-c}(\omega, T_e), \quad (1)$$

where ω is the optical frequency and T_e is the temperature of the conduction electrons in the rod (room temperature, in this case). The first term is the Drude free-electron contribution, with ω_p being the bulk plasmon frequency and γ the plasmon damping rate. The second term is the contribution of transitions between the d band and the conduction band of Au, including transitions at both the X and L points in the Brillouin zone. The real part of the dielectric function is calculated from this imaginary part using the Kramers-Kronig relation. The matrix elements of the interband transitions, as well as the Drude plasmon frequency, are adjusted to reproduce tabulated values of the dielectric functions [26]. The only free parameter in the calculations is the aspect ratio of the rod. An aspect ratio of 5.25 yields a center frequency that matches the experimentally measured value, and is consistent with the rod shapes measured by TEM (see inset of Fig. 1(a)). The linewidth of the calculated spectrum, shown in Fig. 1(a), agrees well with that of the measured spectrum.

Further evidence that we are collecting the scattering from a single rod is provided by the polarization dependence of the scattering, as shown in Fig. 1(b). As the polarization of the incident laser light is rotated, the scattering signal undergoes a nearly complete modulation, characteristic of scattering from a single, oriented dipole.

Having identified individual nanorods, we measure their nonlinearities using a pump-probe technique. The

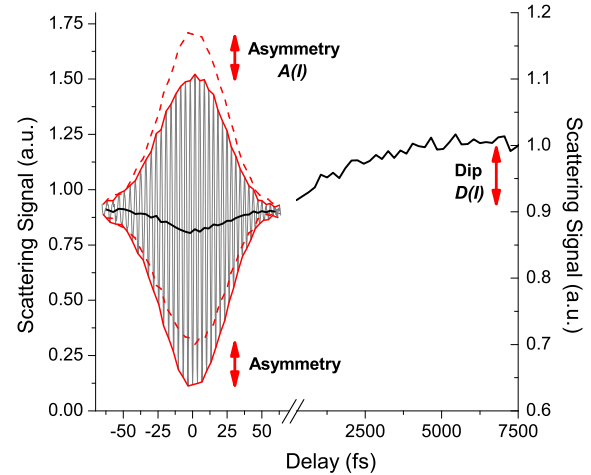


FIG. 2: (Color online) Scattering signal as a function of time delay between the two laser pulses incident on the rod. The light lines on the left-hand side of the figure show the scattering intensity for overlapping pulses with an energy of 47 pJ; also shown (in red online) is the envelope of the interference pattern, and the same envelope, inverted about the average scattering signal at a delay of 75 fs (dashed red line). The heavy line is the average of the upper and lower envelopes. The line on the right-hand side of the figure shows the scattering intensity for non-overlapping pulses with an energy of 94 pJ. Note that both horizontal and vertical scales are different for the two halves of the figure.

rods are excited with 20-fs pulses from a mode-locked, cavity-dumped Ti:Sapphire laser [27]. The pulses are split into two equal-intensity parts, and the delay of one of the pulses is controlled relative to the other by moving a retroreflector, using either a stepper motor (for longer time delays) or a piezoelectric transducer (for shorter time delays). A single lens focuses the two pulses to a common 20- μm spot on the sample. The detected signal is processed by a lock-in amplifier, which is synchronized to a chopper that modulates both laser beams.

We first measure ultrafast nonlinearities by overlapping the two pulses at the rod and varying their relative delay. As shown on the left-hand side of Fig. 2, the measured scattering signal traces out an interference pattern, which exhibits a pronounced asymmetry in intensity. That is, when the laser pulses interfere constructively, the incident intensity is doubled, but the amount of scattering from the rod increases by less than a factor of two, meaning that the scattering cross-section of the rod is lower for the higher intensity. The measured interference patterns do not change as the repetition rate of the laser is varied, indicating that slow, cumulative effects (such as sample heating) do not play a role.

Figure 3(a) shows the power dependence of the measured asymmetry for three different rods. The linear

dependence on laser intensity, I , indicates a third-order nonlinearity; that is, the scattering cross-section can be written as $\sigma(I) = \sigma^{(0)} + I\sigma^{(3)}$. At the highest laser intensities used, the nonlinearity ($I\sigma^{(3)}/\sigma^{(0)}$) is over 20%. If the laser power is increased further, optical damage starts to occur: the scattering signal gradually and irreversibly decreases to a considerably lower value. We believe this reflects changes in the shape of the rod: each laser pulse melts the rod, making it more spherical, thereby shifting the plasmon resonance to higher energies [28].

In order to understand the mechanism for the observed ultrafast nonlinearity, we increase the delay so that the pulses no longer overlap. The right-hand side of Fig. 2 shows a representative result. Fig. 3(b) gives similar results for different laser powers, showing that the recovery time increases as the pump power increases. This effect is characteristic of the heating of conduction electrons by the laser pulse, followed by their cooling and equilibration with lattice phonons [8, 9, 10, 16]. Increasing the delay up to 150 ps results in no detectable change in the scattering signal, indicating that effects related to the heating of lattice phonons are unimportant on the time scales of our measurements.

The results can be modeled as follows. The amount of light transferred from the first (pump) laser pulse to the conduction electrons is determined by calculating the nanorod absorption cross-section; this transferred energy results in a higher electron temperature, T_e . The subsequent evolution of T_e is calculated using a two-temperature model, which treats the conduction electrons and the lattice phonons as two coupled thermal reservoirs [11, 16]. The effect of elevated T_e is to alter the dielectric function for Au, as described by Eqn. 1. The Drude contribution changes due to an increase in the damping rate, $\gamma(T_e)$ [9], while the interband damping increases due to the broadening of the conduction-electron distribution near the Fermi level [23, 24, 25]. Because of the changes in the dielectric function, the plasmon resonance broadens and the resonance frequency shifts. The modified plasmon resonance determines the amount of light scattered from the second (probe) laser pulse. This calculated scattering signal is fit to the data using a single free parameter, which relates the measured laser power to the optical intensity incident on the rod. Fig. 3(b) shows results for three different pump powers from a single rod; equally good agreement was obtained for several other pump powers and for other rods.

The good agreement indicates that electron heating is able to account for the measured nonlinearity on picosecond time scales. Surprisingly, the same model can also explain the measured nonlinearities on femtosecond time scales. More precisely, we can extrapolate the measured thermal nonlinearity for a given laser intensity, I , to zero time delay; this gives a certain “dip” $D(I)$ in the normalized pump-probe signal. (The dip is illustrated for a particular intensity in Fig. 2; in this case, $D(I) \approx 8\%$.)

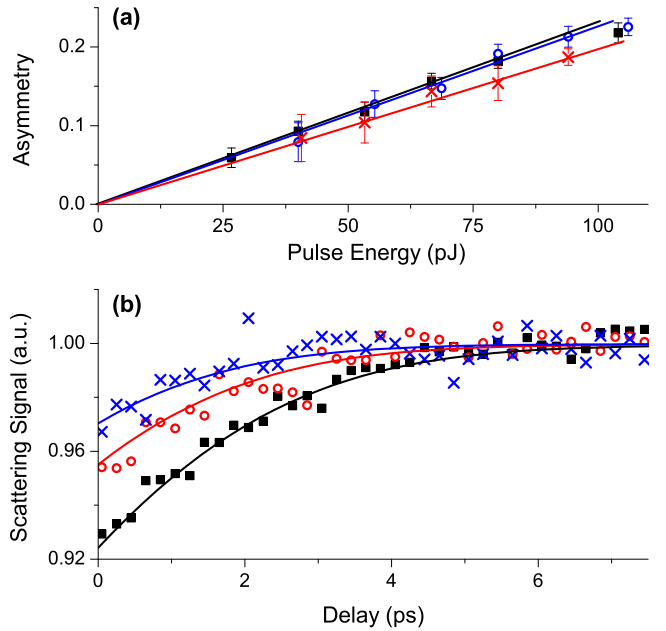


FIG. 3: (Color online) (a) Measured asymmetry in interference patterns for three different rods. (b) The points show the measured scattering signal as a function of the time delay between the two laser pulses incident on the rod, normalized by the measured signal at a delay of 20 ps. The lines are the calculated change in scattering. The three curves, from top to bottom, correspond to pulse energies of 26, 53, and 94 pJ, and are all measured from the same rod.

The measured values of $D(I)$ can be compared to the asymmetries, $A(I)$, of the measured interference patterns, given in Fig. 3(a). If we make the assumption that the only nonlinearity is due to electron heating, and that this nonlinearity is effective even for the shortest time delays, then we obtain a simple relation between the two values:

$$A(I) = 2D(2I). \quad (2)$$

Within our experimental error, we observe exactly this relationship. In other words, we see no change in the dynamics of the nonlinearity as we move from picosecond to femtosecond time scales.

At first glance, this appears to be physically unreasonable, since we do not expect a thermal population of electrons to arise within our 20-fs laser pulse duration. Rather, we expect that the resonant laser pulses directly excite plasmons. Based on the measured resonance linewidth, these plasmons should have a population decay time of at least 7.5 fs. The product of the plasmon decay is expected to be a highly non-thermal electron distribution, which subsequently thermalizes in approximately 200 fs [16, 29]. The nonlinear response due to non-thermal electrons and the response due to coherent plasmons are both expected to be different from that due to a thermal electron population. The relatively

large noise in the single-rod measurements may obscure some of these differences. Nonetheless, the apparent absence of a sizeable ultrafast nonlinearity in excess of the thermal nonlinearity is surprising.

In particular, we expect a substantial nonlinearity associated with the coherent oscillation of the plasmon. For the laser intensities used, we estimate that the amplitude of electron oscillation can reach as much as 8% of the length of the rod. The surfaces of the rod should then restrict the motion of the electrons, producing a significant deviation from harmonic oscillation. Such a surface effect has recently been invoked, for example, to explain third-harmonic generation from quasi-spherical Au nanoparticles [30].

The absence of the coherent plasmon response can be interpreted in two ways. First, there may indeed be a coherent nonlinearity that decays in 7.5 fs, as well as an incoherent nonlinearity of nearly equal magnitude that rises at the same rate, so that the overall effect is nearly constant on ultrafast time scales. Given our experimental errors and the effect of convolution with our 20-fs laser pulses, this explanation would require that the coherent and incoherent nonlinearities be identical to within 11%. Second, strong excitation of the plasmon may reduce the plasmon dephasing time or saturate the plasmon oscillation. For example, strongly driving the plasmon will increase electron-electron and electron-surface scattering rates [16, 29, 31], which will lead to increased plasmon damping.

Our single-rod measurements have established the magnitude of resonant optical nonlinearities in single Au nanorods. The observations lead to the unexpected conclusion that resonant excitation of plasmons results in the same nonlinearity as incoherent excitation of conduction electrons, suggesting previously unrecognized properties of strongly-driven plasmons. Further measurements using shorter pulses may reveal additional dynamics on the few-femtosecond time scale. Alternatively, it may be possible to extend the plasmon lifetime by using nanoparticles made of different metals with lower optical absorbance. The limitation of the measured nonlinearity to approximately 20% means that alternate routes to achieving stronger nonlinearities should be pursued, such as embedding the nanorods in a polarizable medium, or assembling them into ordered structures. We thus believe that our current observation, of significant third-order optical nonlinearities from single Au nanorods, represents a first step towards achieving very large optical nonlinearities on the nanometer scale.

We thank Dr. A. Bakhtyari for valuable assistance. This work was principally supported by the MRSEC program of the NSF under grant No. DMR 0213745, with additional support from the UC-ANL Consortium for Nanoscience Research and from NSF grant No. CHE

0317009. M.P. is supported by the Grainger Postdoctoral Fellowship in Experimental Physics from the University of Chicago.

* Electronic address: pelton@uchicago.edu

- [1] B. E. A. Saleh and M. C. Teich, *Fundamentals of Photonics* (John Wiley & Sons, New York, 1991).
- [2] W. L. Barnes, A. Dereux, and T. W. Ebbesen, *Nature* **424**, 824 (2003).
- [3] S. Nie and S. R. Emory, *Science* **275**, 1102 (1997).
- [4] K. Kneipp *et al.*, *Phys. Rev. Lett.* **78**, 1667 (1997).
- [5] M. Quinten, A. Leitner, J. R. Krenn, and F. R. Aussenegg, *Opt. Lett.* **23**, 1331 (1998).
- [6] S. A. Maier *et al.*, *Nature Materials* **2**, 229 (2003).
- [7] M. J. Feldstein *et al.*, *J. Am. Chem. Soc.* **119**, 6638 (1997).
- [8] J. H. Hodak, A. Henglein, and G. V. Hartland, *J. Phys. Chem. B* **104**, 9954 (2000).
- [9] C. Voisin, N. D. Fatti, D. Christofilos, and F. Vallée, *J. Phys. Chem. B* **105**, 2264 (2001).
- [10] S. Link and M. El-Sayed, *Annu. Rev. Phys. Chem.* **54**, 331 (2003).
- [11] A. Arbouet *et al.*, *Phys. Rev. Lett.* **90**, 177401 (2003).
- [12] T. Itoh, T. Asahi, and H. Masuhara, *Appl. Phys. Lett.* **79**, 1667 (2001).
- [13] Y.-H. Liau, A. N. Unterreiner, Q. Chang, and N. F. Scherer, *J. Phys. Chem. B* **105**, 2135 (2001).
- [14] S. Link *et al.*, *Phys. Rev. B* **61**, 6086 (2000).
- [15] M. Hu *et al.*, *J. Am. Chem. Soc.* **125**, 14925 (2003).
- [16] S. Park, M. Pelton, M. Liu, P. Guyot-Sionnest, and N. Scherer, in preparation.
- [17] C. F. Bohren and D. R. Huffman, *Absorption and Scattering of Light by Small Particles* (John Wiley & Sons, New York, 1983).
- [18] B. Nikoobakht and M. A. El-Sayed, *Chem. Mater.* **15**, 1957 (2003).
- [19] M. Liu and P. Guyot-Sionnest, *J. Phys. Chem. B* **108**, 5882 (2004).
- [20] C. Sönnichsen *et al.*, *Phys. Rev. Lett.* **88**, 077402 (2002).
- [21] H. Jung *et al.*, *Nano Lett.* **4**, 2171 (2004).
- [22] C. Sönnichsen *et al.*, *Appl. Phys. Lett.* **77**, 2949 (2000).
- [23] R. Rosei, F. Antonangeli, and U. M. Grassano, *Surf. Sci.* **37**, 689 (1973).
- [24] R. Rosei, *Phys. Rev. B* **10**, 474 (1974).
- [25] M. Guerrisi, R. Rosei, and P. Winsemius, *Phys. Rev. B* **12**, 557 (1975).
- [26] P. B. Johnson and R. W. Christy, *Phys. Rev. B* **6**, 4370 (1972).
- [27] Y.-H. Liau, A. N. Unterreiner, D. C. Arnett, and N. F. Scherer, *Appl. Opt.* **38**, 7386 (1999).
- [28] S. Link and M. A. El-Sayed, *J. Chem. Phys.* **114**, 2362 (2001).
- [29] W. S. Fann, R. Storz, H. W. K. Tom, and J. Bokor, *Phys. Rev. B* **46**, 13592 (1992).
- [30] M. Lippitz, M. A. van Dijk, and M. Orrit, *Nano. Lett.* **5**, 799 (2005).
- [31] N. Del Fatti *et al.*, *Phys. Rev. B* **61**, 16956 (2000).